1521-0111/12/8202-178–188$25.00
MOLECULAR PHARMACOLOGY
Vol. 82, No. 2
78659/3781370

Mol Pharmacol 82:178–188, 2012

Endomorphin-2: A Biased Agonist at the μ-Opioid Receptor

Guadalupe Rivero, Javier Llorente, Jamie McPherson, Alex Cooke, Stuart J. Mundell, Craig A. McArdle, Elizabeth M. Rosethorne, Steven J. Charlton, Cornelius Krasel, Christopher P. Bailey, Graeme Henderson, and Eamonn Kelly

School of Physiology and Pharmacology (G.R., J.L., J.M., A.C., S.J.M., G.H., E.K.) and School of Clinical Sciences, University of Bristol, Bristol, United Kingdom (C.A.M.); Novartis Institutes for Biomedical Research, Horsham, West Sussex, United Kingdom (E.M.R., S.J.C.); Institute for Pharmacology and Clinical Pharmacy, Marburg, Germany (C.K.); and Department of Pharmacy and Pharmacology, University of Bath, Bath, United Kingdom (C.P.B.)

Received March 15, 2012; accepted May 2, 2012

ABSTRACT

Previously we correlated the efficacy for G protein activation with that for arrestin recruitment for a number of agonists at the μ-opioid receptor (MOPr) stably expressed in HEK293 cells. We suggested that the endomorphins (endomorphin-1 and -2) might be biased toward arrestin recruitment. In the present study, we investigated this phenomenon in more detail for endomorphin-2, using endogenous MOPr in rat brain as well as MOPr stably expressed in HEK293 cells. For MOPr in neurons in brainstem locus ceruleus slices, the peptide agonists [D-Ala^2,*N*-Me-Phe^4,Gly^5-ol]-enkephalin (DAMGO) and endomorphin-2 activated inwardly rectifying K^+ current in a concentration-dependent manner. Analysis of these responses with the operational model of pharmacological agonism confirmed that endomorphin-2 had a much lower operational efficacy for G protein-mediated responses than did DAMGO at native MOPr in mature neurons. However, endomorphin-2 induced faster desensitization of the K^+ current than did DAMGO. In addition, in HEK293 cells stably expressing MOPr, the ability of endomorphin-2 to induce phosphorylation of Ser375 in the COOH terminus of the receptor, to induce association of arrestin with the receptor, and to induce cell surface loss of receptors was much more efficient than would be predicted from its efficacy for G protein-mediated signaling. Together, these results indicate that endomorphin-2 is an arrestin-biased agonist at MOPr and the reason for this is likely to be the ability of endomorphin-2 to induce greater phosphorylation of MOPr than would be expected from its ability to activate MOPr and to induce activation of G proteins.

Introduction

Currently there is much interest in the phenomenon of biased agonism, whereby different agonists at a G protein-coupled receptor (GPCR) can induce the receptor to couple to distinct downstream signaling pathways (Kenakin, 2011; Reiter et al., 2012). The most likely explanation for biased agonism is that different agonists stabilize distinct active conformations of the GPCR (Kahsai et al., 2011), which couple differentially to downstream signaling pathways. One commonly observed form of biased agonism is that between G protein-dependent and arrestin-dependent signaling (Reiter et al., 2012), although there are likely to be many other variations, such as bias in GPCR coupling to different G protein subtypes. The importance of biased agonism is that ligands that could selectively activate certain downstream signaling pathways might be developed, which has the potential to improve the therapeutic potential to manage diseases and to avoid adverse effects.

Agonists at the μ-opioid receptor (MOPr) are extremely important drugs for the management of moderate to severe pain (Corbett et al., 2006), but use of these drugs often leads to undesirable effects, including respiratory depression, constipation, and tolerance, and there is the potential for abuse (Morgan and Christie, 2011). Therefore, there is a need to develop new analgesic drugs with fewer of the unwanted effects associated with classic opioids such as morphine (Corbett et al., 2006).

In a recent study, we investigated the ability of 22 opioid agonists to activate G proteins and to recruit arrestin-3 in HEK293 cells stably expressing MOPr (McPherson et al.,

This work was supported by the National Institutes of Health National Institute on Drug Abuse [Grant DA020836]; the Medical Research Council UK [Grant G0600943]; the Biotechnology and Biochemical Sciences Research Council [Grant BB/D012902/1]; and by a research fellowship from the Basque Government [Grant BFI08.131] (to G.R.).
G.R. and J.L. contributed equally to this work.
Article, publication date, and citation information can be found at http://molpharm.aspetjournals.org.
http://dx.doi.org/10.1124/mol.112.078659.

ABBREVIATIONS: GPCR, G protein-coupled receptor; MOPr, μ-opioid receptor; DAMGO, [D-Ala^2,*N*-Me-Phe^4,Gly^5-ol]-enkephalin; LC, locus ceruleus; GIRK, G protein-coupled, inwardly rectifying, K^+ channel current; β-FNA, β-funaltrexamine; NA, noradrenaline; YFP, yellow fluorescent protein; CFP, cyan fluorescent protein; GRK2, G protein-coupled receptor kinase 2; DAPI, 4′,6-diamidino-2-phenylindole dihydrochloride; GTPγS, guanosine 5′-*O*-(γ-thiotriphosphate); HA, hemagglutinin; FRET, fluorescence resonance energy transfer.

2010). We showed that there was a strong correlation between the two signaling outputs for most of those agonists; however, there seemed to be bias toward arrestin recruitment for a few agonists, particularly the endomorphins. Because arrestins are implicated in signaling as well as GPCR regulation (Shenoy and Lefkowitz, 2011), this finding might have important consequences for the ability of new ligands based on the endomorphin structure to induce a different array of responses, compared with older, morphine-like drugs.

Endomorphin-1 (Tyr-Pro-Trp-Phe-NH_2) and endomorphin-2 (Tyr-Pro-Phe-Phe-NH_2) are opioid peptides with high affinity and selectivity for the MOPr (Zadina et al., 1997). Although the peptides were originally identified in extracts from mammalian brain (Zadina et al., 1997), investigators' inability to identify a precursor protein for either of these peptides has raised the question of whether they function as endogenous opioids in the mammalian central nervous system (Corbett et al., 2006; Terskiy et al., 2007). Analogs of these peptides have potential as novel analgesic agents, and one such drug, Cyt-1010, is reported to be in development (http://www.cytogelpharma.com/news.html).

The purpose of this study was to determine whether endomorphin-2 is a biased agonist at MOPr. Our data indicate that endomorphin-2 is biased toward arrestin recruitment over G protein activation. Furthermore, we show that the likely source for the arrestin bias is the ability of endomorphin-2 to induce greater phosphorylation of MOPr than would be predicted from the ability of this peptide to activate G protein-coupled responses.

Materials and Methods

Drugs. Morphine hydrochloride was obtained from Mcfarlan Smith (Edinburgh, UK), etorphine from Research Triangle Institute (Research Triangle Park, NC), and DAMGO from Bachem (Bubendorf, Switzerland). Noradrenaline, β-funaltrexamine (β-FNA), prazosin, and cocaine were obtained from Sigma-Aldrich (Gillingham, UK). Endomorphin-2 and chelerythrine were obtained from Tocris Bioscience (Bristol, UK).

Brain Slice Preparation. Male Wistar rats (130–170 g) were killed through cervical dislocation, and horizontal brain slices (200–250 μm thick) containing the locus ceruleus (LC) were prepared as described previously (Bailey et al., 2003). All experiments were performed in accordance with the UK Animals (Scientific Procedures) Act of 1986, the European Communities Council Directive of 1986 (86/609/EEC), and the University of Bristol ethical review documents.

Whole-Cell Patch-Clamp Recordings. Slices were submerged in a slice chamber (0.5 ml) mounted on a microscope stage and were superfused (2.5–3 ml/min) with artificial cerebrospinal fluid composed of 126 mM NaCl, 2.5 mM KCl, 1.2 mM $MgCl_2$, 2.4 mM $CaCl_2$, 1.2 mM NaH_2PO_4, 11.1 mM D-glucose, 21.4 mM $NaHCO_3$, and 0.1 mM ascorbic acid, saturated with 95% O_2/5% CO_2 at 33–34°C. For patch-clamp recordings, LC neurons were observed with Nomarski optics by using infrared light and individual cell somata were cleaned with a gentle flow of artificial cerebrospinal fluid from a pipette. Whole-cell voltage-clamp recordings (V_h = −60 mV) were made by using electrodes (3–6 MΩ) filled with a solution containing 115 mM potassium gluconate, 10 mM HEPES, 11 mM EGTA, 2 mM $MgCl_2$, 10 mM NaCl, 2 mM MgATP, and 0.25 mM Na_2GTP (pH 7.3; osmolarity, 270 mOsM). Recordings of whole-cell currents were filtered at 2 kHz by using an Axopatch 200B amplifier (Molecular Devices, Sunnyvale, CA) and were analyzed off-line by using pClamp (Molecular Devices). Activation of MOPr evoked a transmembrane K^+ current and, with the use of whole-cell patch-clamp recordings, a real-time index of MOPr activation could be recorded continually. The opioid-evoked current was continuously recorded at a holding potential of −60 mV. MOPrs and α_2-adrenoceptors couple to the same set of K^+ channels in LC neurons (North and Williams, 1985). To reduce variations between cells, the amplitudes of opioid-evoked currents were normalized to the maximal α_2-adrenoceptor-mediated current in the same cell evoked by 100 μM noradrenaline (NA) applied in the presence of 1 μM prazosin and 3 μM cocaine.

All drugs were applied in the superfusing solution at known concentrations. Concentration-response curves for MOPr agonists were obtained through cumulative addition. To reduce the influence of desensitization on the slopes and maxima of the curves, each concentration of drug was added for only 2 min, by which time the response had reached a steady state. Each individual cell was exposed to a limited number of high concentrations (greater than the EC_{50}) of the drug and to one supramaximal concentration. The maximal response for each drug obtained in this way was not different from the maximal response observed in other cells exposed to a single supramaximal concentration of that drug. For example, the amplitude of the maximum of the cumulative concentration-response curve for etorphine was 123.0 ± 11.1% (n = 3) of the response to 100 μM NA, whereas that evoked by a single, maximally effective concentration of etorphine (1 μM) was 142.4 ± 14.3% (n = 4) of the response to 100 μM NA (unpaired t test, p = 0.36).

Cell Culture. HEK293 cells were maintained at 37°C, in 95% O_2/5% CO_2, in Dulbecco's modified Eagle's medium (Invitrogen, Carlsbad, CA) supplemented with 10% fetal bovine serum, 10 U/ml penicillin, and 10 mg/ml streptomycin. In addition, the culture medium for the HEK293 cells stably expressing MOPr tagged at the NH_2 terminus with HA contained 250 μg/ml G-418 (Geneticin; PAA Laboratories GmbH, Pasching, Austria).

Ser375 Phosphorylation. Agonist-induced phosphorylation of MOPr at Ser375 was assessed by using an IN Cell Analyzer 1000 high-content imaging platform (GE Healthcare, Chalfont St. Giles, Buckinghamshire, UK), as described previously (Caunt et al., 2010), with minor variations. Cells cultured in 96-well plates were incubated with different concentrations of various MOPr agonists for 10 min at 37°C. Cells were then fixed, permeabilized, and immunostained with rabbit anti-phospho-Ser375 polyclonal antibody (1:1000 dilution; Cell Signaling Technology, Danvers, MA), followed by incubation with Alexa Fluor 488-conjugated goat anti-rabbit antibody (Invitrogen) and 4′,6-diamidino-2-phenylindole dihydrochloride (DAPI) nuclear stain (600 nM). Images were acquired and then analyzed with IN Cell Investigator software (Workstation 3.5; GE Healthcare), with a dual area object analysis algorithm. Fluorescence from DAPI staining was used to define the nuclear area and thus the presence of a cell. The intensities of the Alexa 488 fluorescence in the whole-cell areas of the observed cells were averaged, and these values were used for further analysis. Alexa 488 fluorescence intensity values, which indicated phosphorylation of Ser375 at the MOPr, underwent background subtraction and then were normalized to the values obtained with phosphate-buffered saline (basal) and with 100 μM DAMGO.

For Western blotting, cells were washed three times with ice-cold phosphate-buffered saline after agonist treatment and were lysed in immunoprecipitation buffer (50 mM Tris, pH 7.5, 10 mM EDTA, 150 mM NaCl, 0.5% deoxycholate, 0.1% SDS, 1% Nonidet P-40, 50 mM NaF, 10 mM glycerol-2-phosphate, 200 μM sodium orthovanadate, 25 mM sodium pyrophosphate, and 1× complete mini-protease inhibitor; Roche Diagnostics, Indianapolis, IN). Cell lysates were clarified through centrifugation at 12,000 rpm at 4°C in a microcentrifuge and underwent immunoprecipitation with anti-HA antibody (HA-11; 3 μg per sample; Covance Research Products, Princeton, NJ) and protein G/A-agarose overnight at 4°C. Beads were washed three times with immunoprecipitation buffer, and proteins were eluted with the addition of SDS-sample buffer for 3 min at 95°C. Proteins were then resolved through 8% SDS-polyacrylamide gel electrophoresis and were transferred to polyvinylidene difluoride membranes. Membranes were incubated with the anti-phospho-Ser375 polyclonal

antibody (1:1000). Blots were stripped and reprobed with anti-HA antibody (HA-11; 1:1000). Signal detection was performed with enhanced chemiluminescence methods.

FRET Experiments. These experiments were performed exactly as described previously (McPherson et al., 2010). HEK293 cells cotransfected with MOPr-yellow fluorescent protein (YFP), arrestin-3-cyan fluorescent protein (CFP), and G protein-coupled receptor kinase 2 (GRK2) (this increased the agonist-induced FRET signal obtained) were plated on poly-L-lysine-coated glass coverslips. Cells were mounted on a Nikon Eclipse TE2000S inverted microscope (Nikon, Melville, NY) and were observed by using an oil-immersion 63× lens, a Polychrome V monochromator for excitation, and a dual-emission photometric system (TILL Photonics, Gräfelfing, Germany). MOPr agonists were applied by using a computer-assisted superfusion system. Fluorescence was measured at 535 ± 15 nm (F_{YFP}) and 480 ± 20 nm (F_{CFP}) after excitation at 436 ± 10 nm. Signals detected by avalanche photodiodes were digitized by using an analog/digital converter (Digidata 1322A; Molecular Devices), and data were stored on a personal computer with Axoscope 9.2 (Molecular Devices). FRET was calculated as the F_{YFP}/F_{CFP} ratio. Off-line analyses of the FRET (F_{YFP}/F_{CFP}) data were performed to determine the kinetics and extent of the MOPr-YFP and arrestin-3-CFP interactions induced by different agonists.

Cell Surface Receptor Loss. Receptor loss was assessed with enzyme-linked immunosorbent assays, as described previously (McPherson et al., 2010). HEK293 cells stably expressing HA-tagged MOPr were seeded into 24-well tissue culture dishes coated with 0.1 mg/ml poly-L-lysine, 24 h before experimentation. For time course experiments, cells were washed and then challenged for 0 to 30 min at 37°C with Dulbecco's modified Eagle's medium containing opioid agonist. Reactions were terminated by fixing the cells with 3.7% formaldehyde. Cells were then incubated with primary antibody (anti-HA-11, 1:1000) for 1 h at room temperature. For investigations of the agonist concentration dependence of internalization, cells were prelabeled with primary antibody for 1 h at 4°C before incubation with the agonists for 30 min at 37°C. Cells were then incubated with secondary antibody (goat anti-mouse antibody conjugated with alkaline phosphatase, 1:1000; Sigma-Aldrich), a colorimetric alkaline phosphatase substrate (Bio-Rad Laboratories, Hemel Hempstead, UK) was added, and samples were assayed at 405 nm in a microplate reader. Changes in surface receptor expression were determined by normalizing data from each treatment group to corresponding control surface receptor levels determined from cells not exposed to opioid agonist, and values were expressed as either percentage of surface receptor expression or cell surface loss (as percentage of no-drug control), depending on the primary antibody labeling method used, with the background signal from HEK293 cells being subtracted from all receptor-transfected cell values. All experiments were performed in triplicate.

Data Analyses. All data were analyzed by using GraphPad Prism (GraphPad Software Inc., San Diego, CA). Agonist concentration-response data from LC neurons were fitted to sigmoidal curves with variable slopes, with the bottom of the curve in each case being constrained to 0, for determination of agonist EC_{50} and E_{max} values and for graphical representation of the data. Parameters from this fitting were then used as initial values for fitting of the concentration-response data to the operational model of pharmacological agonism (Black and Leff, 1983; Bailey et al., 2009; McPherson et al., 2010), $E = E_m\tau^n[A]^n/(K_a + [A])^n + \tau^n[A]^n$, where the response E is expressed in terms of the molar concentration of agonist A, the theoretical maximal effect E_m (greater than that which can be functionally attained) (Black and Leff, 1983), the equilibrium dissociation constant K_a, the transducer ratio τ, and n, which is the slope of the curve (n in this equation is not the same as the Hill slope, although the values may be similar). E_m and n are intrinsic properties of the receptor/cell and are independent of the agonist used, whereas τ depends on the cell, receptor function, and agonist used. For each pair of curves (i.e., concentration-response curves for DAMGO, etorphine, and endomorphin-2 in the presence and absence of 30 nM β-funaltrexamine), values for E_m, K_a, and n (shared for the paired curves for each agonist) and for τ were determined.

For graphical representation of Ser375 phosphorylation, concentration-response data were fitted to sigmoidal curves with variable slopes, with the bottom of the curve in each case being constrained to 0. Parameters from this fitting were then used as initial values for fitting of the concentration-response data to the operational model of pharmacological agonism (see above). For operational model fitting, constrained parameters were E_m shared and <101, n shared and <2.0, and K_a values determined previously (McPherson et al., 2010), which were as follows: DAMGO, 228 nM; etorphine, 3.5 nM; endomorphin-2, 283 nM; morphine, 250 nM.

Ser375 phosphorylation data were also analyzed for efficacy values with the method described previously (Ehlert, 1985), $e = (E_{max,agonist}/E_{max,full\ agonist}) \times [(K_{a,agonist}/EC_{50,agonist}) + 1] \times 0.5$, where e is the efficacy of the test agonist, $E_{max,agonist}$ and $E_{max,full\ agonist}$ are the relative maximal response values of the test agonist and an agonist yielding a full response, respectively, and K_a and EC_{50} are the equilibrium dissociation constant and EC_{50}, respectively, for the test agonist. The efficacy values for agonist-induced cell surface loss were also determined with this method.

For occupancy-response relationships, data from McPherson et al., 2010 were reanalyzed to calculate fractional receptor occupancy at each concentration of agonist used in [^{35}S]GTPγS or arrestin-3 recruitment assays. The fractional receptor occupancy was calculated by using the expression $p = [D]/(Ka + [D])$, where p is the fractional receptor occupancy (between 0 and 1), [D] is the agonist concentration, and K_a is the equilibrium dissociation constant, the value of which was determined previously in membranes of these cells (McPherson et al., 2010).

For desensitization in LC neurons, the desensitization-phase data (up to 10 min) from individual experiments were combined and fitted to a one-phase, exponential-decay model to obtain values for $t_{1/2}$ and the rate constant k for decay, as well as maximal desensitization (plateau level). For analysis of FRET data, the $t_{1/2}$ of the MOPr-YFP/arrestin-3-CFP interaction was obtained by fitting the data from the time points at which the agonist had been applied to a one-phase, exponential-association model. The extent of the agonist-induced MOPr-YFP and arrestin-3-CFP interaction was calculated as the peak of the interaction and was normalized to the interaction induced by the subsequent application of 10 μM DAMGO.

For ligand bias calculations, the method described by Rajagopal et al. (2011) was used with previously generated data (McPherson et al., 2010). For each agonist with either G protein activation or arrestin-3 recruitment, the "effective signaling" (σ_{lig}) was calculated, where $\sigma_{lig} = \log(\tau_{lig}/\tau_{ref})$; τ_{lig} is the operational eficacy of a ligand for a particular signaling pathway, and τ_{ref} is the operational efficacy for the reference agonist (assumed to be unbiased) for that pathway. In this case, the reference ligand was Leu-enkephalin (McPherson et al., 2010). The bias factor (β_{lig}) for a particular ligand was then calculated as follows: $\beta_{lig} = (\sigma_{lig}^{path1} - \sigma_{lig}^{path2})/\sqrt{2}$. Statistical differences were determined, where appropriate, with Student's t test, one-sample t test, or F test for comparison of different models (the simpler model was selected unless the extra sum-of-squares F test had a p value of <0.05), by using GraphPad Prism.

Results

Relative Operational Efficacy of Agonists at Native MOPr in Mature Neurons. Previously we reported that, in HEK293 cells stably expressing MOPr, endomorphin-1 and -2 may be biased toward arrestin recruitment over G protein coupling (McPherson et al., 2010). To investigate whether endomorphins show bias at endogenous MOPrs in mature neurons, we needed a reliable measure of MOPr agonist efficacy for a G protein-mediated response in LC neurons.

Therefore, we compared the ability of several MOPr agonists to activate G protein-coupled, inwardly rectifying, K^+ channel current (GIRK) in individual rat LC neurons. We constructed concentration-response curves for endomorphin-2, DAMGO, and etorphine, before and after exposure of the brain slices to the irreversible MOPr antagonist β-FNA (30 nM, 30 min). In the absence of β-FNA, all three agonists produced the same maximal responses, which indicates that, for this response in this tissue, endomorphin-2 is a full agonist (Fig. 1). Pretreatment with β-FNA shifted the agonist concentration-response curve for each of these agonists to the right and depressed the maximal response (Fig. 1). The calculated mean ± S.E.M. values for the sigmoidal curve fitting are listed in Supplemental Table 1.

The curves for each agonist in the absence and presence of β-FNA were then fitted to the equation describing the operational model of pharmacological agonism (Black and Leff, 1983) (see *Materials and Methods*), and values of operational efficacy (τ) were obtained. Relative efficacy values are given in Table 1, and calculated mean ± S.E.M. values are listed in Supplemental Table 2. In a previous study, we obtained a τ value of 1.6 for morphine in LC neurons (Bailey et al., 2009). We and others reported previously that the maximal response for morphine is lower than that for the other agonists (Osborne and Williams, 1995; Bailey et al., 2009), which confirms that it is a partial agonist and must have lower efficacy than the other three agonists for this response. The rank order of τ values (Table 1) obtained from LC neurons (DAMGO > etorphine ≫ endomorphin-2 > morphine) was similar to that obtained previously with these agonists for GTPγS binding in HEK293 cells (McPherson et al., 2010) (Table 1), which indicates that the relative operational efficacy of G protein-dependent signaling for these agonists is independent of the tissue in which the MOPr is expressed. These data demonstrated that, for MOPr-G protein coupling in both a heterologous cell line and mature neurons, endomorphin-2 had much lower efficacy than DAMGO.

Rate and Extent of Agonist-Induced Desensitization of MOPr-Activated K^+ Current in LC Neurons. We next assessed the ability of the MOPr agonists to induce acute desensitization of the GIRK current in LC neurons (Fig. 2). A receptor-saturating concentration of each agonist was applied for 10 min and the GIRK current was recorded. Representative traces for each agonist are shown in Fig. 2. It can be seen that DAMGO, etorphine, and endomorphin-2 induced extensive rapid desensitization of the GIRK current, whereas morphine induced less desensitization over the same period. The desensitization phase for each agonist was fitted to a one-phase, exponential-decay model to determine the rate of desensitization and the maximal amount of desensitization. The data are shown in Fig. 2 and Table 2. The fastest rate of desensitization was observed with endomorphin-2 (F test, $p < 0.0001$), with the order from faster to slower decay rate constant k values being as follows: endomorphin-2 (0.440 min^{-1}) > DAMGO (0.233 min^{-1}) > morphine (0.205 min^{-1}) > etorphine (0.137 min^{-1}). The ability of a number of other MOPr agonists to induce acute desensitization in LC cells was examined, but none induced faster desensitization than endomorphin-2 (Supplemental Fig. 1). These data indicate that, in rat brain neurons, the ability of endomorphin-2 to induce rapid desensitization is much greater than would be predicted from its efficacy for GIRK activation.

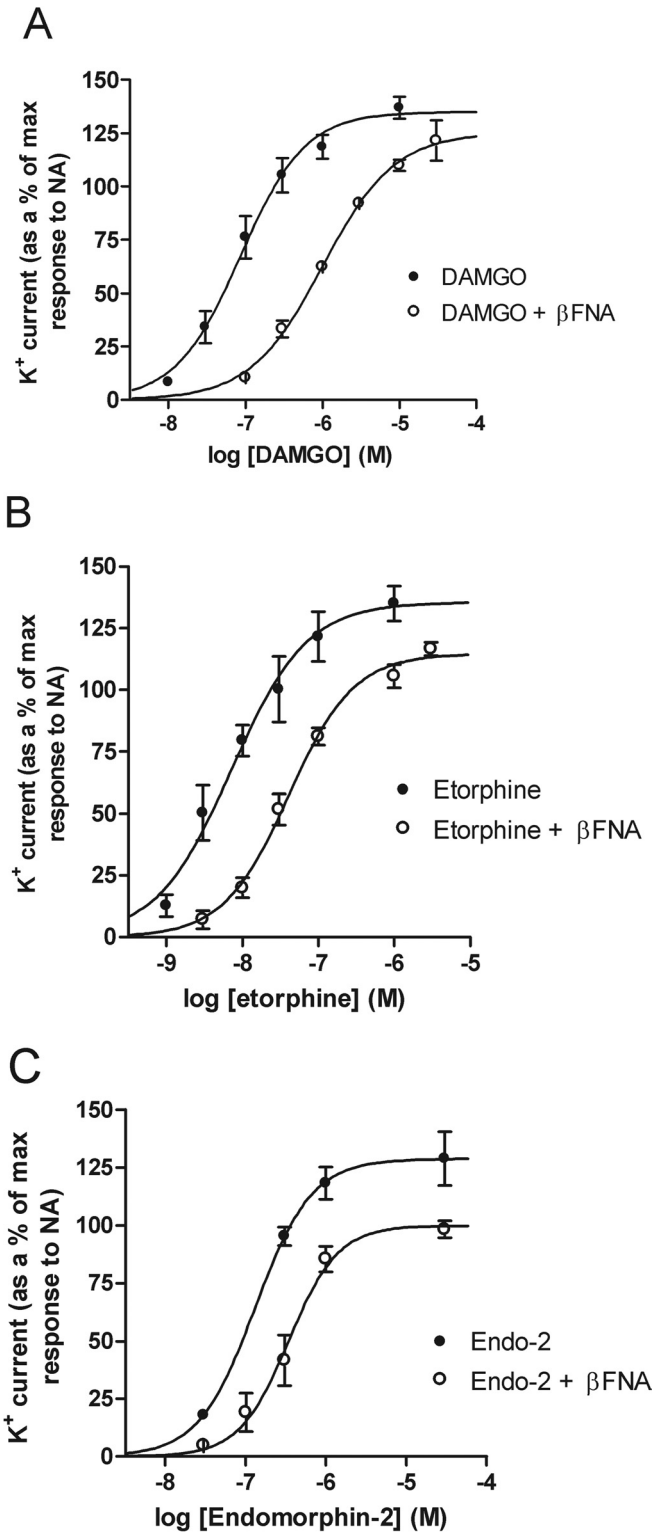

Fig. 1. Concentration-response curves for activation of the GIRK current in rat LC neurons by DAMGO, etorphine, and endomorphin-2. In individual LC neurons, concentration-response curves for DAMGO (n = 3–5) (A), etorphine (n = 3–8) (B),and endomorphin-2 (Endo-2) (n = 3–5) (C) were determined before and after treatment with the irreversible MOPr antagonist β-FNA (30 nM) for 30 min, with normalization to the maximal current induced by NA (100 μM) in the same neuron. Each concentration of agonist was applied until the response reached a steady state (~2 min). Different concentrations were tested on each neuron to ensure that the responses to higher concentrations of agonist were not attenuated by desensitization. For graphical representation, the data were fitted to sigmoidal concentration-response curves with variable slopes.

TABLE 1

Comparison of relative efficacy values for different agonist-induced responses at MOPr

Values refer either to relative operational efficacy (τ) calculated by using the operational model or to relative efficacy (e) calculated according to the method described under *Materials and Methods*. In each case, the actual value of τ or e for DAMGO in each assay is shown in parentheses. For relative efficacy calculations, the DAMGO value was set to 1.00 in each case.

Assay	Relative Efficacy			
	DAMGO	Etorphine	Endomorphin-2	Morphine
GIRK current activation (τ), LC neurons	1.00 (100.5)	0.43	0.07	0.02[a]
GTPγS binding (τ), HEK293 cells	1.00 (28.5)[b]	0.40[b]	0.18[b]	0.18[b]
Ser375 phosphorylation (τ), HEK293 cells	1.00 (1.99)	0.92	0.92	0.44
Ser375 phosphorylation (e), HEK293 cells	1.00 (0.66)	0.83	0.97	0.52
Arrestin-3 recruitment (τ), HEK293 cells	1.00 (0.82)[b]	0.98[b]	1.02[b]	0.26[b]
Cell surface receptor loss (e), HEK293 cells	1.00 (0.71)	0.70	0.68	0.34

[a] Value was calculated from data reported by Bailey et al. (2009).
[b] Values were taken from the report by McPherson et al. (2010).

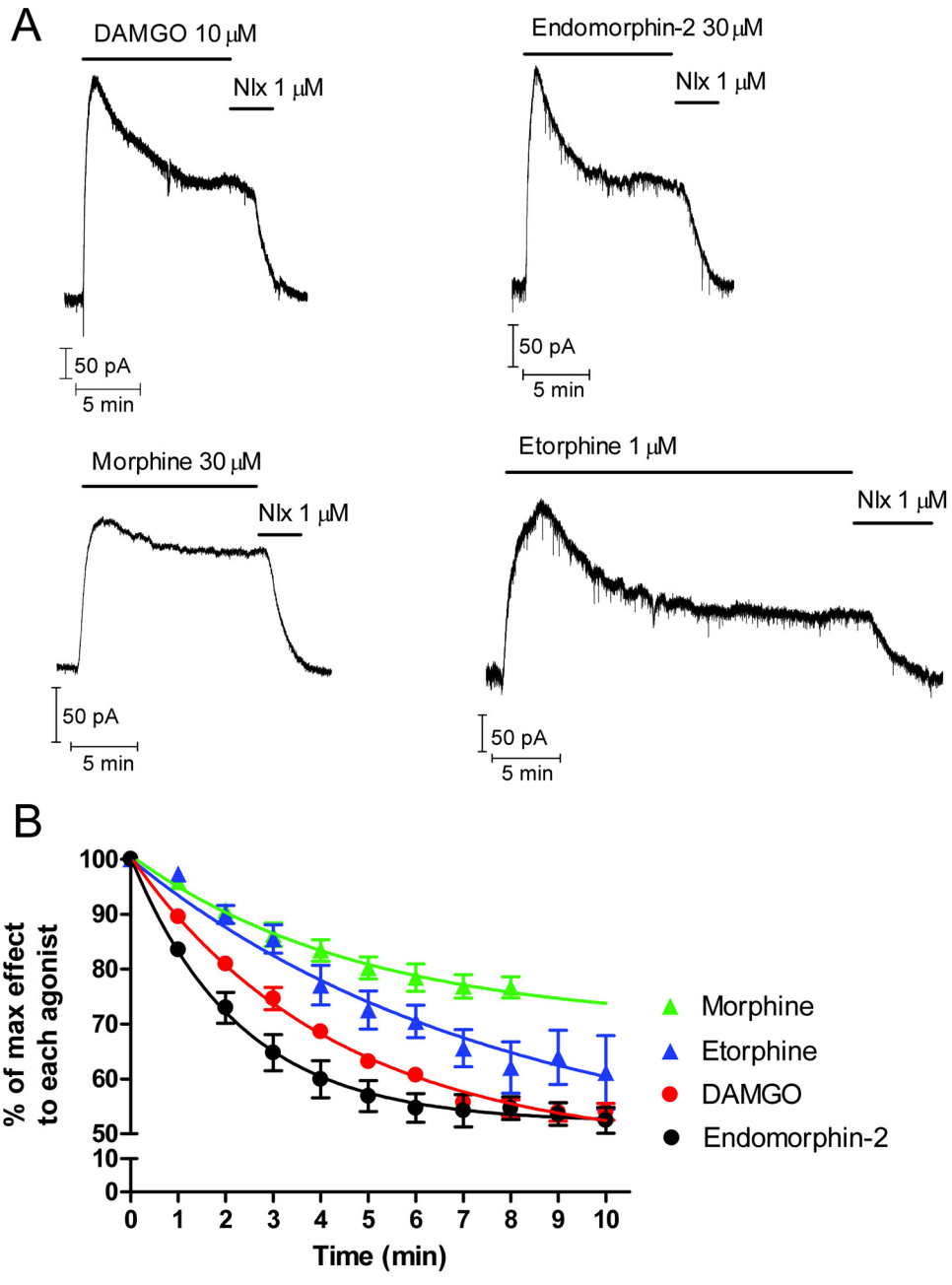

Fig. 2. Rate and extent of desensitization of MOPr-evoked GIRK channel currents in rat LC neurons. A, outward potassium currents were recorded from single LC neurons, clamped at −60 mV, in response to application of saturating concentrations of DAMGO (10 μM), endomorphin-2 (30 μM), morphine (30 μM), and etorphine (1 μM). Agonists, which were applied for at least 10 min, induced an outward current that was not sustained for the period of drug application (solid bars) but decreased (desensitization) to a steady state (plateau). Desensitization to etorphine was slow and needed longer to reach the plateau. The opioid receptor antagonist naloxone (Nlx) (1 μM) was perfused immediately after each agonist, to restore the basal level. B, desensitization-phase data from 3 to 10 neurons for each agonist were best fitted to a one-phase, exponential-decay model (one- and two-phase, exponential-decay models were compared with an F test for each data set). The fastest rate of desensitization observed was for endomorphin-2. Values shown are mean ± S.E.M.

TABLE 2

Agonist-induced desensitization of MOPr-activated GIRK current in LC neurons

The desensitization-phase data for a saturating concentration of each agonist from a number of experiments (Fig. 2B) were fitted to a one-phase, exponential-decay model, to obtain values for $t_{1/2}$ and the extent of desensitization (plateau). Values shown are means and 95% confidence intervals.

Agonist	$t_{1/2}$ (95% CI)	Extent of Desensitization (95% CI)
	min	%
Endomorphin-2 (30 μM)	1.58 (1.52–1.64)	47.9 (47.4–48.4)
DAMGO (10 μM)	2.98 (2.76–3.23)	52.7 (51.1–54.3)
Etorphine (1 μM)	5.04 (4.10–6.55)	54.6 (47.4–61.8)
Morphine (30 μM)	3.38 (3.16–3.63)	30.2 (29.1–31.3)

CI, confidence interval.

Agonist-Induced Phosphorylation of MOPr at Ser375. MOPr agonists induce phosphorylation at Ser375 in the COOH terminus of the receptor, and an antiphosphoreceptor antibody was developed to identify this phosphorylation event (Schulz et al., 2004). To facilitate measurement of agonist-induced MOPr phosphorylation at Ser375, automated imaging of permeabilized HEK293 cells was undertaken (Fig. 3A). Initial experiments indicated that this Ser375 phosphorylation was mediated in part by GRK2, was independent of protein kinase C activation, and partly depended on coupling to G proteins (Supplemental Fig. 2). Concentration-response curves for phosphorylation of Ser375 in response to 10 min of agonist stimulation were constructed. DAMGO, endomorphin-2, and etorphine seemed to be full agonists in this assay, whereas morphine was a partial agonist (Fig. 3B; see Supplemental Table 3 for parameters for fitting of data to sigmoidal curves). Etorphine was the most potent agonist, followed by DAMGO and endomorphin-2 and then morphine. These agonist effects were confirmed with Western blotting of MOPr immunoprecipitated from HEK293 cells (Fig. 3C). Concentration-response data obtained from the automated imaging were then subjected to operational analysis with the binding constants for MOPr in HEK293 cells determined in our previous study (McPherson et al., 2010). Relative efficacy values are given in Table 1, and calculated mean ± S.E.M. values are listed in Supplemental Table 4. They indicate that, unlike the results from G protein coupling, the operational efficacy of endomorphin-2 for phosphorylation of Ser375 in MOPr was similar to that of etorphine and almost as high as that of DAMGO. The operational efficacy for morphine remained low in this assay. Because the operational analysis of these data produced τ values with large standard errors (Supplemental Table 4), the method described by Ehlert (1985) was used as an alternative approach to determine relative efficacy in this assay; this method uses a combination of EC_{50}, maximal response, and binding constant values (for details, see *Materials and Methods*) to obtain a measure of efficacy (e). This produced a similar rank order of relative efficacy (Table 1), compared with the operational analysis. Whichever method was used to determine relative efficacy from these data, the efficacy of endomorphin-2 for Ser375 phosphorylation was close to that of DAMGO, although the latter had much higher efficacy for G protein activation.

Agonist-Induced Interaction of MOPr with Arrestin-3. We used FRET assays to assess the MOPr/arrestin-3 interaction in intact cells after agonist application. HEK293 cells were transiently transfected with MOPr-YFP and arrestin-3-CFP; 48 h later, FRET was monitored for 3 to 5 min

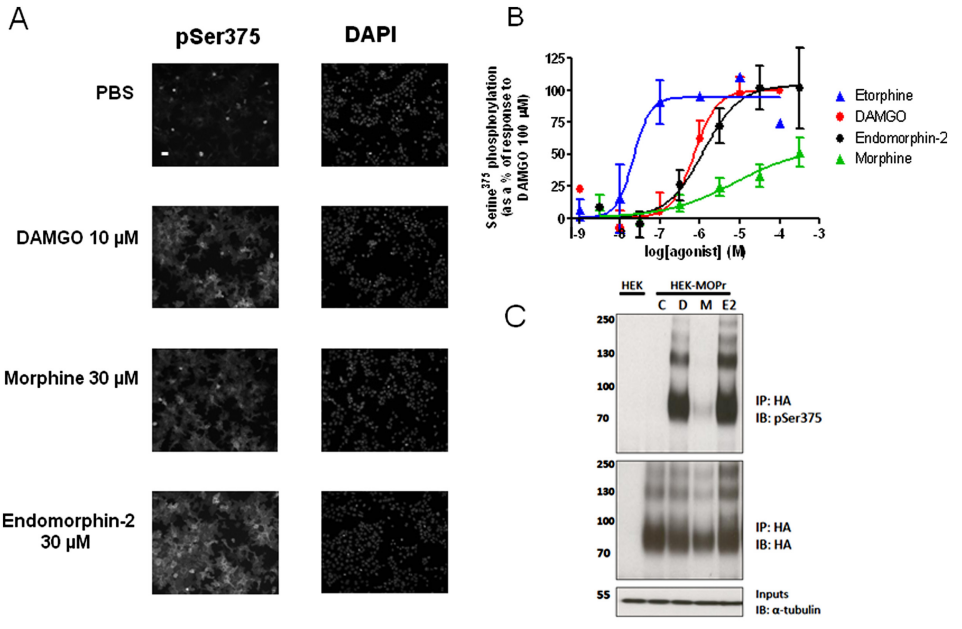

Fig. 3. Image-based quantification of agonist-induced phosphorylation of Ser375 in MOPr. HEK293 cells stably expressing HA-tagged MOPr were plated in 96-well plates and were exposed to different concentrations of MOPr agonists for 10 min. Cells were then fixed and used for immunocytochemical staining with an anti-phospho-Ser375 antibody, and image analysis was performed as described under *Materials and Methods*. A, representative images of the Ser375-phosphorylated MOPr immunofluorescence signal and the DAPI staining in untreated cells [phosphate-buffered saline (PBS)] and cells treated with DAMGO (10 μM), morphine (30 μM), or endomorphin-2 (30 μM) are shown. Cells in the mitotic process showed high nonspecific immunofluorescence signal levels. Scale bar, 30 μm. Results shown are representative of three to six independent experiments. B, concentration-response curves for Ser375 phosphorylation. Values are mean ± S.E.M. of three to six independent experiments. C, Western blot of phospho-Ser375-MOPr immunoprecipitated from HEK293 cells with anti-HA antibody and identified with anti-phospho-Ser375 antibody. Endomorphin-2 (E2) (30 μM) induced phosphorylation of Ser375 similar to that induced by DAMGO (D) (10 μM) and much greater than that induced by morphine (M) (30 μM). C, control; IP, immunoprecipitation; IB, immunoblotting.

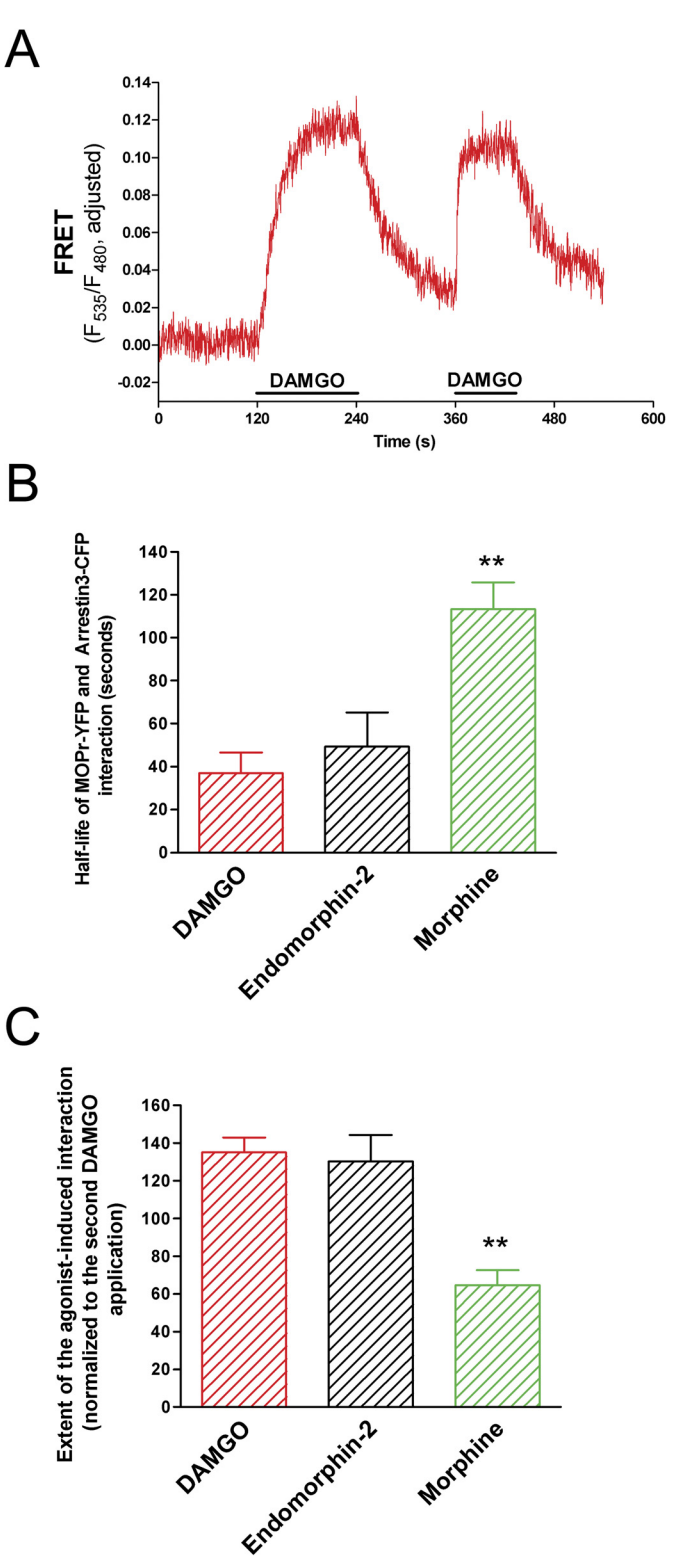

Fig. 4. Agonist-induced interaction of MOPr with arrestin-3, as measured in FRET experiments. HEK293 cells were transiently transfected with MOPr-YFP, GRK2, and arrestin-3-CFP. A, FRET trace for DAMGO (10 μM). An increase in the FRET ratio (measured as F_{535}/F_{480}) reflects the interaction between MOPr-YFP and arrestin-3-CFP. B, half-life of MOPr-YFP/arrestin-3-CFP interaction after addition of 10 μM DAMGO, 30 μM endomorphin-2, or 30 μM morphine. FRET traces were fitted to a one-phase, exponential model for calculation of $t_{1/2}$. Values are mean ± S.E.M. from at least three separate experiments in each case. **, $P < 0.01$, Student's t test, $t_{1/2}$ for morphine was significantly longer than that for DAMGO or endomorphin-2. C, extent of agonist-induced FRET. The maximal FRET for each agonist was expressed as a percentage of that induced with subsequent addition of 10 μM DAMGO. The value for DAMGO is greater than 100% because the second DAMGO response was always slightly less than the first (see results in A). Values are mean ± S.E.M. from at least three separate experiments in each case. **, $P < 0.01$, Student's t test, value for morphine was significantly lower than that for DAMGO or endomorphin-2.

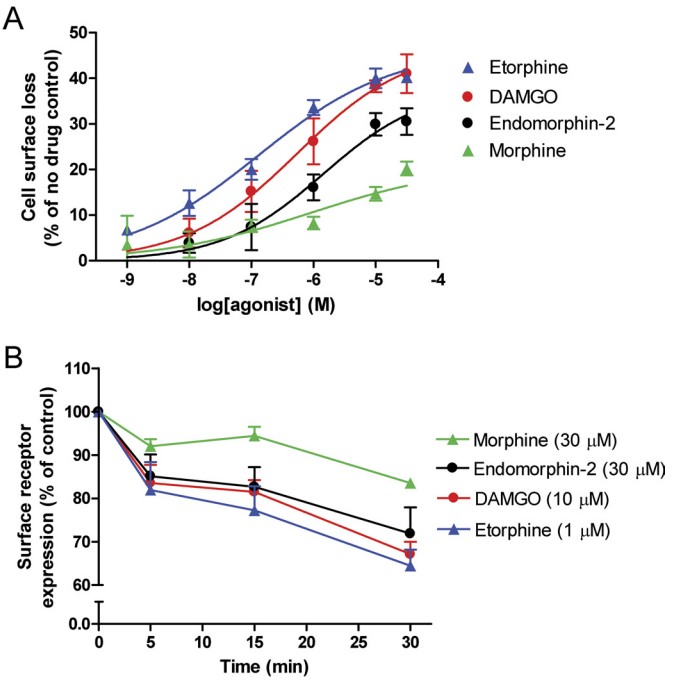

Fig. 5. Concentration- and time-dependent cell surface loss of MOPr from HEK293 cells stably expressing HA-tagged MOPr. A, cells were incubated with different concentrations of agonist for 30 min before determination of cell surface MOPr loss with enzyme-linked immunosorbent assays. Data were fitted to sigmoidal curves with variable slopes. Values are mean ± S.E.M. from four separate experiments, each performed in triplicate. B, cells were incubated with receptor-saturating concentrations of agonist (morphine, 30 μM; endomorphin-2, 30 μM; DAMGO, 10 μM; etorphine, 1 μM) for up to 30 min for determination of time-dependent cell surface MOPr loss. Values are mean ± S.E.M. from three to five separate experiments, each performed in triplicate.

after the addition of DAMGO (10 μM), etorphine (10 μM), endomorphin-2 (30 μM), or morphine (30 μM). With the exception of etorphine, which did not wash out, in each case DAMGO (10 μM) was added after the first drug had been washed out, to obtain a relative measure of maximal response (Fig. 4A). Analysis of agonist-induced FRET showed that the $t_{1/2}$ of the MOPr/arrestin-3 association-induced FRET was relatively low for DAMGO and endomorphin-2 and much higher for morphine (Fig. 4B). Furthermore, DAMGO and endomorphin-2 produced rapid increases in the FRET ratio that were of similar maximal amplitudes, whereas morphine produced a smaller increase in the FRET ratio, compared with the other agonists (Fig. 4C).

Agonist-Induced Cell Surface Loss of MOPr. The ability of DAMGO, etorphine, endomorphin-2, and morphine to induce loss of cell surface MOPr was assessed with enzyme-linked immunosorbent assays. Both the agonist concentration and time dependence of cell surface loss were assessed (Fig. 5). The agonist concentration-response curves indicated that etorphine was the most potent agonist, followed by DAMGO and then morphine and endomorphin-2. Receptor-saturating concentrations of DAMGO, etorphine, and endo-

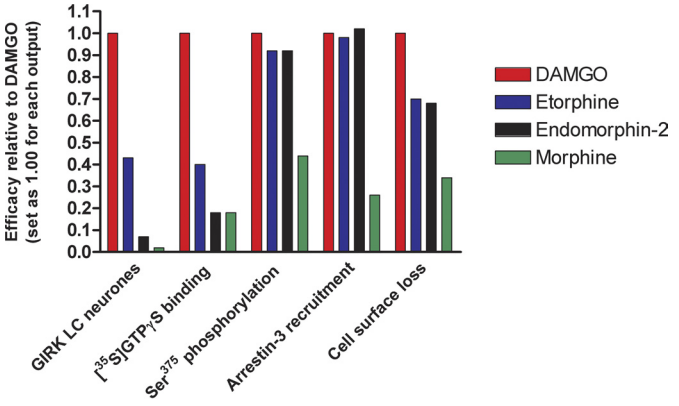

Fig. 6. Relative efficacy values for DAMGO, etorphine, endomorphin-2, and morphine for five MOPr signaling outputs. Values refer to efficacy relative to that of DAMGO, which was set to 1.00 for each output. The values for [^{35}S]GTPγS binding and arrestin-3 recruitment were taken from Table 2 of McPherson et al. (2010). The efficacy values are τ values for operational efficacy in each case except for cell surface loss, for which the values are relative efficacy (e) values obtained with the method described by Ehlert (1985). The τ value for morphine in the GIRK assay was obtained from Bailey et al. (2009). Actual values of efficacy for DAMGO in each assay are given in Table 1.

morphin-2, applied for 30 min, each induced >25% loss of cell surface MOPr (Fig. 5B); a saturating concentration of morphine induced less extensive loss of MOPr (<15%). The parameters for fitting the concentration-response data to sigmoidal curves are shown in Supplemental Table 5. It was not possible to fit the data in Fig. 5A with the operational model, even with a range of constraints; therefore, the relative efficacies were calculated with the method described by Ehlert (1985). In this analysis (Table 1), the rank order of relative efficacy (e) values was DAMGO > etorphine = endomorphin-2 > morphine. Together these results show that, although endomorphin-2 had an operational efficacy value for G protein coupling/K^+ current activation much lower than that of DAMGO, it was able to induce cell surface loss of MOPr almost the same as that produced by DAMGO. Furthermore, although endomorphin-2 and morphine had comparable low values of operational efficacy for [^{35}S]GTPγS binding in HEK293 cell studies, endomorphin-2 induced more extensive cell surface loss of MOPr than did morphine.

Comparison of Agonist Efficacy Values for Multiple Signaling Outputs. For comparison of relative efficacy values from multiple signaling outputs, efficacy values for each response analyzed in this study are presented as a bar graph in Fig. 6, with the efficacy of DAMGO set as 1 in each case. The results show that the relative efficacy values of the agonists for GIRK activation and [^{35}S]GTPγS binding (i.e., G protein responses) closely mirrored each other, with endomorphin-2 having low efficacy relative to DAMGO. In contrast, the efficacy of endomorphin-2 relative to DAMGO was much higher for phosphorylation of Ser375, arrestin-3 recruitment, and cell surface loss. For Ser375 phosphorylation and arrestin-3 recruitment, the efficacy of endomorphin-2 was essentially the same as that of DAMGO.

Agonist Occupancy-Response Relationships. For further examination of the agonist-induced responses to the four MOPr agonists, occupancy-response relationships were constructed for MOPr agonists by using previously generated data (McPherson et al., 2010) for [^{35}S]GTPγS binding and arrestin-3 recruitment assays for receptors stably expressed

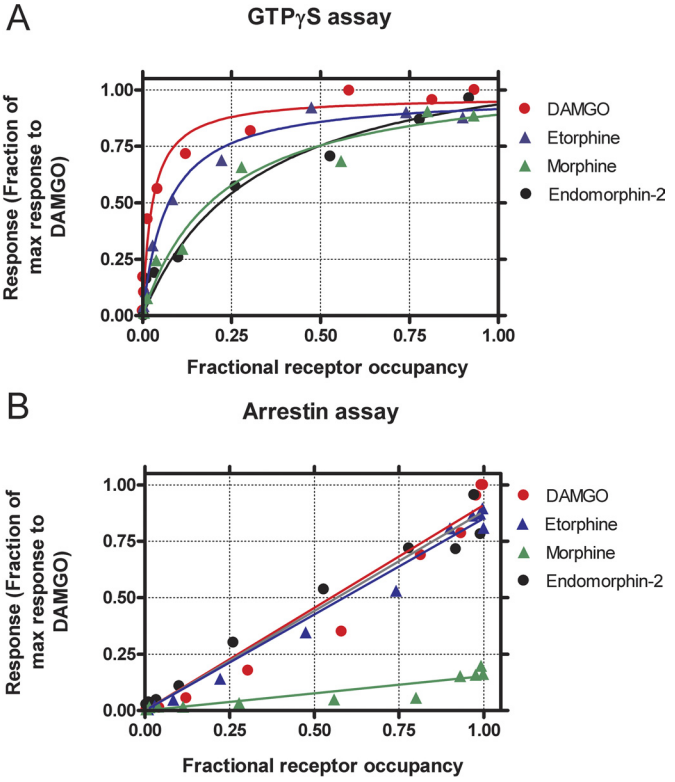

Fig. 7. Fractional receptor occupancy-response relationships for MOPr agonists. Previously published (McPherson et al., 2010) concentration-response data for agonist-induced [^{35}S]-GTPγS binding and arrestin-3 recruitment were used to determine the occupancy-response relationships for MOPr agonists. Fractional receptor occupancy at each concentration of agonist was calculated as described under *Materials and Methods*. A, relationship between [^{35}S]GTPγS binding and fractional receptor occupancy for DAMGO, etorphine, morphine, and endomorphin-2. Data were fitted to a one-site binding model (hyperbola) with GraphPad Prism; the r^2 value for each was >0.964. Data points represent the mean response at each level of occupancy. B, relationship between arrestin-3 recruitment and fractional receptor occupancy for DAMGO, etorphine, morphine, and endomorphin-2. Data were fitted with linear regression because this yielded a better fit than a one-site binding model (hyperbola). Data points represent the mean response at each level of occupancy.

in HEK293 cells (Fig. 7). Transformation of the data in this way enables examination of the agonist occupancy-response relationship without the complication of binding affinity. These results show that the efficacy order for coupling to G protein was DAMGO > etorphine > endomorphin-2 = morphine (Fig. 7A) (comparing agonist responses at occupancies of 0.25, for example), whereas that for arrestin-3 recruitment was DAMGO = etorphine = endomorphin-2 ≫ morphine (Fig. 7B). It is also clear that the relationship between fractional MOPr occupancy and arrestin-3 recruitment was essentially linear, which suggests a lack of amplification in this response. Of interest, analysis of Ser375 phosphorylation and internalization data suggested that the relationships between fractional receptor occupancy and these outputs were also linear (Supplemental Fig. 3). The occupancy-response relationship in Fig. 7B might suggest that it is morphine rather than endomorphin-2 that is unusual, because the arrestin response-fractional receptor occupancy relationship for morphine lies apart from those of the other three agonists. To investigate this, we used previously published data to construct occupancy-response relationships for other agonists that had similar operational efficacies in the GTPγS

assay (McPherson et al., 2010), including morphine and endomorphin-2, as well as oxycodone, 6-monoacetylmorphine, and morphine-6-glucuronide. When the occupancy-response relationships for arrestin-3 recruitment were plotted for this group of agonists, it could be clearly seen that endomorphin-2 had much higher efficacy than any of the other agonists within this group (Supplemental Fig. 4). This strongly supports the conclusion that endomorphin-2 is an arrestin-biased ligand.

Calculation of Ligand Bias. A method to quantify ligand bias has been described (Rajagopal et al., 2011). With this method, operational efficacy (τ) values are calculated for a series of agonists for two signaling outputs and are compared with the τ values for an agonist that is unbiased between the two signaling pathways being assessed (see *Materials and Methods*). On the basis of previous data, we concluded that Leu-enkephalin is an unbiased agonist (McPherson et al., 2010). By using this approach, we calculated bias for the MOPr ligands that yielded significant responses in the two assays, which enabled us to calculate bias for 16 of the 22 ligands investigated in our previous study. Calculation of ligand bias indicated that endomorphin-2 was significantly biased toward arrestin-3 recruitment (Fig. 8). Although no other ligands displayed statistically significant bias, it is worth noting that endomorphin-1, etorphine, and alfentanil displayed trends toward arrestin bias, whereas DAMGO displayed a trend toward G protein bias.

Discussion

Previous studies on the endomorphins identified these peptides as selective MOPr agonists with relatively high affinity for the receptor (Zadina et al., 1997). The endomorphins were reported to be partial agonists at MOPr in some cases, such as in GTPγS binding assays with spinal cord and thalamus (Hosohata et al., 1998; Narita et al., 1998; Xie et al., 2008) and in inhibition of neuronal Ca^{2+} currents (Connor et al., 1999), whereas the endomorphins behaved as full agonists in other cases, such as inhibition of contraction of mouse vas deferens (Al-Khrasani et al., 2001; Rónai et al., 2006); such differences are likely to depend in part on the receptor reserve in each tissue. In the present study with LC neurons, we found endomorphin-2 to be a full agonist for activation of GIRK current. However, the receptor reserve for the endomorphin-2 response in LC neurons was less than those for DAMGO and etorphine, because limited receptor depletion with a low concentration (30 nM) of β-FNA led to a greater reduction in the maximal response to endomorphin-2 (22% reduction) than in those to DAMGO (7% reduction) and etorphine (15% reduction), as well as a smaller shift in agonist EC_{50} (2.6-fold for endomorphin-2, 5.6-fold for etorphine, and 11.5-fold for DAMGO). To quantify the efficacy of endomorphin-2 relative to DAMGO and other MOPr agonists, we used the MOPr inactivation method that we (Bailey et al., 2009) and others (Rónai et al., 2006; Madia et al., 2009) used previously to determine agonist efficacy. In this analysis, we determined that the operational efficacy of endomorphin-2 for activation of GIRK was only 7% of that of DAMGO, with etorphine having an intermediate efficacy. These relative values reflect those obtained for GTPγS binding in membranes of HEK293 cells stably expressing MOPr, where the efficacy value for endomorphin-2 was 17% of that for DAMGO, with etorphine again exhibiting an intermediate value (McPherson et al., 2010). Because the MOPr-mediated activation of GIRK in LC neurons is a G protein-mediated response, it is perhaps not surprising that the relative efficacies in the two assays are similar.

Previous studies (Yu et al., 1997; Virk and Williams, 2008) suggested that the ability of saturating concentrations of MOPr agonists to induce acute (0–10-min) desensitization is agonist efficacy-dependent. On this basis, endomorphin-2 would be predicted to induce relatively little desensitization of MOPr-mediated GIRK activation during this relatively short period of agonist exposure, because of its lower efficacy for this effect. However, endomorphin-2-induced desensitization was as extensive and occurred more rapidly than that induced by DAMGO. The desensitization induced by morphine and etorphine was slower than that induced by DAMGO and was in line with efficacy values determined in this study for LC neurons and for [^{35}S]GTPγS binding assays with HEK293 cells (McPherson et al., 2010). The acute desensitization induced by endomorphin-2 may be partly attributable to the ability of this ligand to induce efficient arrestin recruitment to MOPr, leading to extensive uncoupling of receptor and G protein. This cannot be the full explanation, however, because the efficacy of endomorphin-2 for arrestin-3 recruitment in HEK293 cells was the same as those of DAMGO and etorphine (McPherson et al., 2010) but acute desensitization was faster with endomorphin-2. One possibility is that the low efficacy and consequent small receptor reserve of endomorphin-2 for GIRK activation, coupled with relatively high efficacy for arrestin recruitment, may make it particularly sensitive to the onset of acute desensitization. In contrast, DAMGO is an agonist with high efficacy for GIRK activation and consequently a large receptor reserve, which would display slower desensitization because, although it induces efficient arrestin recruitment to MOPr, the high efficacy for GIRK activation means that a much

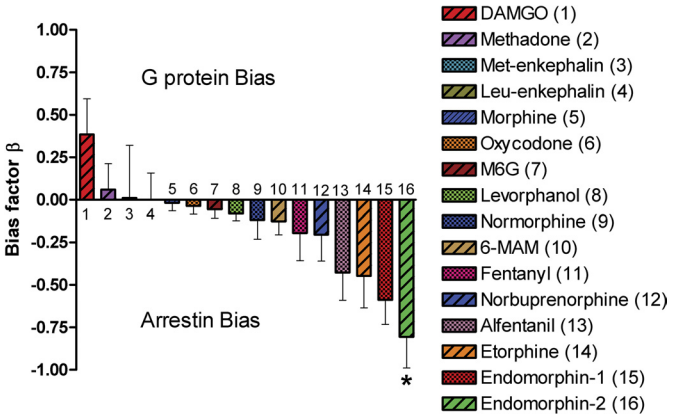

Fig. 8. Calculation of ligand bias at MOPr. The bias factor for 16 MOPr ligands was calculated as described under *Materials and Methods*, using data for ligand-induced [^{35}S]GTPγS binding and arrestin-3 recruitment previously generated in HEK293 cells stably expressing MOPr (McPherson et al., 2010). Leu-enkephalin was selected as the reference unbiased ligand on the basis of its position when operational efficacy values for the two signaling outputs were plotted (see Fig. 3 of McPherson et al., 2010). For each agonist with either G protein activation or arrestin-3 recruitment, the effective signaling (σ_{lig}) was calculated as $\sigma_{lig} = \log(\tau_{lig}/\tau_{ref})$; the bias factor ($\beta_{lig}$) for a particular ligand was then calculated as $\beta_{lig} = (\sigma_{lig}^{path1} - \sigma_{lig}^{path2})/\sqrt{2}$. A one-sample, two-tailed t test was used to determine whether the degree of bias was statistically different from 0. *, endomorphin-2 displayed a statistically significant level of bias ($p < 0.05$). M6G, morphine-6-glucuronide; 6-MAM, 6-monoacetylmorphine.

greater loss of functional receptors, compared with endomorphin-2, would be required to yield significant desensitization of the GIRK response.

Differences in arrestin-2 versus arrestin-3 recruitment have not been explored to date, and it is possible that the profile of arrestin-2 versus arrestin-3 recruitment to the endomorphin-2-occupied MOPr is different from that induced by other agonists, leading to agonist- and arrestin-dependent signaling and regulation that are distinct from those of other agonists. Such a scenario was described recently for arrestin isoform interactions with MOPr in response to DAMGO and morphine (Groer et al., 2011). The precise role of arrestins in MOPr regulation in neurons remains to be fully elucidated. Although MOPr desensitization by high-efficacy agonists such as DAMGO is arrestin-dependent in cell lines (Chu et al., 2008), the acute desensitization induced by Met-enkephalin was unaffected in LC neurons from arrestin-3-knockout mice (Dang et al., 2011; Quillinan et al., 2011). These studies suggest that arrestins play a complex role in MOPr function in neurons, with recovery from acute desensitization being much faster in neurons from arrestin-3-knockout mice (Dang et al., 2011; Quillinan et al., 2011). Given that MOPr dephosphorylation can occur at the cell surface (Arttamangkul et al., 2006; Doll et al., 2011), arrestin interaction and internalization might actually reduce the rate of MOPr resensitization, which might be manifested as an enhanced rate of desensitization, as observed in our LC neuron study.

In additional studies, we investigated the ability of the agonists DAMGO, etorphine, endomorphin-2, and morphine to induce phosophorylation of Ser375 in the COOH-terminal tail of MOPr, to recruit arrestin-3 to MOPr in intact cells through FRET, and to induce cell surface loss of MOPr. We reasoned that the ability of endomorphin-2 to recruit arrestin-3 effectively might be attributable to more-rapid or more-extensive MOPr phosphorylation at Ser375. Although we (McPherson et al., 2010) and others (Yu et al., 1997) previously compared the ability of receptor-saturating concentrations of agonist to promote MOPr phosphorylation, in the current study we were able to construct full concentration-response curves for Ser375 phosphorylation, which allowed estimates of relative agonist efficacy to be made. This revealed that the efficacy of endomorphin-2 to induce Ser375 phosphorylation in MOPr was similar to that of DAMGO and much higher than that of morphine. This suggests that it is actually the ability of endomorphin-2 to promote phosphorylation of MOPr efficiently that underlies its ability to recruit arrestin-3 to MOPr and also to induce MOPr internalization to a greater extent than morphine. Recent studies indicated that MOPr is phosphorylated on multiple residues in the COOH terminus (Doll et al., 2011; Lau et al., 2011) (S. Oldfield, A. Butcher, A. Tobin, G. Henderson, and E. Kelly, unpublished observations) and the pattern of phosphorylation is agonist-dependent. Ser375 is undoubtedly a key residue in terms of arrestin recruitment (Schulz et al., 2004) but other residues may be important for arrestin recruitment (Lau et al., 2011), and it will be of particular interest to determine the ability of the endomorphins to induce phosphorylation of individual residues in the COOH terminus of MOPr. This does not explain, however, why endomorphin-2 induces more-efficient MOPr phosphorylation than morphine. Given that biased agonism suggests that different agonists can stabilize distinct active conformations of a GPCR (Kahsai et al., 2011), it is possible that endomorphin-2 stabilizes a conformation of the MOPr that couples relatively poorly to G proteins but is readily phosphorylated by kinases such as GRK2 or possibly kinases distinct from those that phosphorylate the DAMGO- or morphine-occupied MOPr.

The distinction between endomorphin-induced MOPr signaling and trafficking can be deduced from careful analysis of previous studies, in which [^{35}S]GTPγS binding assays revealed the endomorphins to have low efficacy values close to those of morphine (Hosohata et al., 1998; Narita et al., 1998; Sim et al., 1998; Xie et al., 2008) but the endomorphins were able to induce efficient trafficking of MOPr under conditions where morphine was ineffective (Burford et al., 1998; McConalogue et al., 1999; Trafton et al., 2000). The advantages of quantifying efficacy with full concentration-response curves and of examining occupancy-response relationships are that such differences can be observed more clearly and can be quantified. Previous studies often used saturating concentrations of agonist to compare efficacies, which is of limited use for comparison of the efficacies of full agonists. In addition, comparison of potencies and maximal responses (intrinsic activity) sometimes does not reveal biased agonism (Molinari et al., 2010). More-sophisticated approaches to quantifying ligand bias have been proposed (Rajagopal et al., 2011), and the application of one such approach to our data from HEK293 cells (Fig. 8) identified the arrestin bias of endomorphin-2 as statistically significant.

In conclusion, endomorphin-2 is an arrestin-biased MOPr agonist, and this may be explained by the drug's ability to promote efficient phosphorylation of the receptor. Future studies will be focused on determining whether the pattern of MOPr phosphorylation induced by endomorphin-2 is different from that of other agonists, such as DAMGO and morphine. Endomorphin-related ligands are reported to have favorable profiles in terms of analgesia and tolerance/dependence and seem to produce less respiratory depression than other agonists (J. E. Zadina, unpublished data). It remains to be seen whether such profiles are attributable to the behavior of the endomorphins as arrestin-biased ligands at MOPr.

Authorship Contributions

Participated in research design: Mundell, McArdle, Rosethorne, Charlton, Krasel, Bailey, Henderson, and Kelly.

Conducted experiments: Rivero, Llorente, McPherson, and Cooke.

Contributed new reagents or analytic tools: McArdle and Krasel.

Performed data analysis: Rivero, Llorente, McPherson, Cooke, Mundell, McArdle, and Kelly.

Wrote or contributed to the writing of the manuscript: Mundell, McArdle, Rosethorne, Charlton, Krasel, Bailey, Henderson, and Kelly.

References

Al-Khrasani M, Orosz G, Kocsis L, Farkas V, Magyar A, Lengyel I, Benyhe S, Borsodi A, and Rónai AZ (2001) Receptor constants for endomorphin-1 and endomorphin-1-ol indicate differences in efficacy and receptor occupancy. *Eur J Pharmacol* **421:**61–67.

Arttamangkul S, Torrecilla M, Kobayashi K, Okano H, and Williams JT (2006) Separation of mu-opioid receptor desensitization and internalization: endogenous receptors in primary neuronal cultures. *J Neurosci* **26:**4118–4125.

Bailey CP, Couch D, Johnson E, Griffiths K, Kelly E, and Henderson G (2003) Mu-opioid receptor desensitization in mature rat neurons: lack of interaction between DAMGO and morphine. *J Neurosci* **23:**10515–10520.

Bailey CP, Llorente J, Gabra BH, Smith FL, Dewey WL, Kelly E, and Henderson G (2009) Role of protein kinase C and mu-opioid receptor (MOPr) desensitization in tolerance to morphine in rat locus coeruleus neurons. *Eur J Neurosci* **29:**307–318.

Black JW and Leff P (1983) Operational models of pharmacological agonism. *Proc R Soc Lond B Biol Sci* **220:**141–162.

Burford NT, Tolbert LM, and Sadee W (1998) Specific G protein activation and

mu-opioid receptor internalization caused by morphine, DAMGO and endomorphin I. *Eur J Pharmacol* **342:**123–126.
Caunt CJ, Armstrong SP, and McArdle CA (2010) Using high-content microscopy to study gonadotrophin-releasing hormone regulation of ERK. *Methods Mol Biol* **661:**507–524.
Chu J, Zheng H, Loh HH, and Law PY (2008) Morphine-induced mu-opioid receptor rapid desensitization is independent of receptor phosphorylation and beta-arrestins. *Cell Signal* **20:**1616–1624.
Connor M, Schuller A, Pintar JE, and Christie MJ (1999) Mu-opioid receptor modulation of calcium channel current in periaqueductal grey neurons from C57B16/J mice and mutant mice lacking MOR-1. *Br J Pharmacol* **126:**1553–1558.
Corbett AD, Henderson G, McKnight AT, and Paterson SJ (2006) 75 years of opioid research: the exciting but vain quest for the Holy Grail. *Br J Pharmacol* **147 (Suppl 1):**S153–S162.
Dang VC, Chieng B, Azriel Y, and Christie MJ (2011) Cellular morphine tolerance produced by βarrestin-2-dependent impairment of μ-opioid receptor resensitization. *J Neurosci* **31:**7122–7130.
Doll C, Konietzko J, Pöll F, Koch T, Höllt V, and Schulz S (2011) Agonist-selective patterns of μ-opioid receptor phosphorylation revealed by phosphosite-specific antibodies. *Br J Pharmacol* **164:**298–307.
Ehlert FJ (1985) The relationship between muscarinic receptor occupancy and adenylate cyclase inhibition in the rabbit myocardium. *Mol Pharmacol* **28:**410–421.
Groer CE, Schmid CL, Jaeger AM, and Bohn LM (2011) Agonist-directed interactions with specific beta-arrestins determine mu-opioid receptor trafficking, ubiquitination, and dephosphorylation. *J Biol Chem* **286:**31731–31741.
Hosohata K, Burkey TH, Alfaro-Lopez J, Varga E, Hruby VJ, Roeske WR, and Yamamura HI (1998) Endomorphin-1 and endomorphin-2 are partial agonists at the human mu-opioid receptor. *Eur J Pharmacol* **346:**111–114.
Kahsai AW, Xiao K, Rajagopal S, Ahn S, Shukla AK, Sun J, Oas TG, and Lefkowitz RJ (2011) Multiple ligand-specific conformations of the β_2-adrenergic receptor. *Nat Chem Biol* **7:**692–700.
Kenakin T (2011) Functional selectivity and biased receptor signaling. *J Pharmacol Exp Ther* **336:**296–302.
Lau EK, Trester-Zedlitz M, Trinidad JC, Kotowski SJ, Krutchinsky AN, Burlingame AL, and von Zastrow M (2011) Quantitative encoding of the effect of a partial agonist on individual opioid receptors by multisite phosphorylation and threshold detection. *Sci Signal* **4**:ra52.
Madia PA, Dighe SV, Sirohi S, Walker EA, and Yoburn BC (2009) Dosing protocol and analgesic efficacy determine opioid tolerance in the mouse. *Psychopharmacology* (*Berl*) **207:**413–422.
McConalogue K, Grady EF, Minnis J, Balestra B, Tonini M, Brecha NC, Bunnett NW, and Sternini C (1999) Activation and internalization of the mu-opioid receptor by the newly discovered endogenous agonists, endomorphin-1 and endomorphin-2. *Neuroscience* **90:**1051–1059.
McPherson J, Rivero G, Baptist M, Llorente J, Al-Sabah S, Krasel C, Dewey WL, Bailey CP, Rosethorne EM, Charlton SJ, et al. (2010) μ-Opioid receptors: correlation of agonist efficacy for signalling with ability to activate internalization. *Mol Pharmacol* **78:**756–766.
Molinari P, Vezzi V, Sbraccia M, Grò C, Riitano D, Ambrosio C, Casella I, and Costa T (2010) Morphine-like opiates selectively antagonize receptor-arrestin interactions. *J Biol Chem* **285:**12522–12535.
Morgan MM and Christie MJ (2011) Analysis of opioid efficacy, tolerance, addiction and dependence from cell culture to human. *Br J Pharmacol* **164:**1322–1334.
Narita M, Mizoguchi H, Oji GS, Tseng EL, Suganuma C, Nagase H, and Tseng LF (1998) Characterization of endomorphin-1 and -2 on [^{35}S]GTPγS binding in the mouse spinal cord. *Eur J Pharmacol* **351:**383–387.
North RA and Williams JT (1985) On the potassium conductance increased by opioids in rat locus coeruleus neurones. *J Physiol* **364:**265–280.
Osborne PB and Williams JT (1995) Characterization of acute homologous desensitization of mu-opioid receptor-induced currents in locus coeruleus neurones. *Br J Pharmacol* **115:**925–932.
Quillinan N, Lau EK, Virk M, von Zastrow M, and Williams JT (2011) Recovery from mu-opioid receptor desensitization after chronic treatment with morphine and methadone. *J Neurosci* **31:**4434–4443.
Rajagopal S, Ahn S, Rominger DH, Gowen-MacDonald W, Lam CM, Dewire SM, Violin JD, and Lefkowitz RJ (2011) Quantifying ligand bias at seven-transmembrane receptors. *Mol Pharmacol* **80:**367–377.
Reiter E, Ahn S, Shukla AK, and Lefkowitz RJ (2012) Molecular mechanism of β-arrestin-biased agonism at seven-transmembrane receptors. *Annu Rev Pharmacol Toxicol* **52:**179–197.
Rónai AZ, Al-Khrasani M, Benyhe S, Lengyel I, Kocsis L, Orosz G, Tóth G, Kató E, and Tóthfalusi L (2006) Partial and full agonism in endomorphin derivatives: comparison by null and operational model. *Peptides* **27:**1507–1513.
Schulz S, Mayer D, Pfeiffer M, Stumm R, Koch T, and Höllt V (2004) Morphine induces terminal micro-opioid receptor desensitization by sustained phosphorylation of serine-375. *EMBO J* **23:**3282–3289.
Shenoy SK and Lefkowitz RJ (2011) β-Arrestin-mediated receptor trafficking and signal transduction. *Trends Pharmacol Sci* **32:**521–533.
Sim LJ, Liu Q, Childers SR, and Selley DE (1998) Endomorphin-stimulated [^{35}S]GTPγS binding in rat brain: evidence for partial agonist activity at mu-opioid receptors. *J Neurochem* **70:**1567–1576.
Terskiy A, Wannemacher KM, Yadav PN, Tsai M, Tian B, and Howells RD (2007) Search of the human proteome for endomorphin-1 and endomorphin-2 precursor proteins. *Life Sci* **81:**1593–1601.
Trafton JA, Abbadie C, Marek K, and Basbaum AI (2000) Postsynaptic signaling via the μ-opioid receptor: responses of dorsal horn neurons to exogenous opioids and noxious stimulation. *J Neurosci* **20:**8578–8584.
Virk MS and Williams JT (2008) Agonist-specific regulation of mu-opioid receptor desensitization and recovery from desensitization. *Mol Pharmacol* **73:**1301–1308.
Xie H, Woods JH, Traynor JR, and Ko MC (2008) The spinal antinociceptive effects of endomorphins in rats: behavioral and G protein functional studies. *Anesth Analg* **106:**1873–1881.
Yu Y, Zhang L, Yin X, Sun H, Uhl GR, and Wang JB (1997) Mu opioid receptor phosphorylation, desensitization, and ligand efficacy. *J Biol Chem* **272:**28869–28874.
Zadina JE, Hackler L, Ge LJ, and Kastin AJ (1997) A potent and selective endogenous agonist for the mu-opiate receptor. *Nature* **386:**499–502.

Address correspondence to: Dr. Eamonn Kelly, School of Physiology and Pharmacology, University of Bristol, University Walk, Bristol BS8 1TD, UK. E-mail: e.kelly@bristol.ac.uk